

# Hydriding and dehydriding properties of $Mg_2Ni/Ni$ and $Mg_2Ni/Ni + 5 \text{ wt.}\% \text{ Cu}$ prepared by mechanical alloying

A.F. Palacios-Lazcano<sup>a,\*</sup>, J.G. Cabañas-Moreno<sup>a</sup>, J. Bonifacio-Martínez<sup>b</sup>,  
J.L. Iturbe-García<sup>b</sup>, F. Cruz-Gandarilla<sup>a</sup>, H.A. Calderón<sup>a</sup>

<sup>a</sup> Instituto Politécnico Nacional – ESFM – Departamento de Ciencia de Materiales,  
Apartado Postal 21-408, 07300, México, D.F., México.

<sup>b</sup> Instituto Nacional de Investigaciones Nucleares, Departamento de Química,  
Km. 36.5 Carr. México-Toluca, 52045, Salazar, México.

Recibido el 6 de febrero de 2009; aceptado el 18 de agosto de 2009

Elemental powders of Mg, Ni and Cu are subjected to high-energy ball milling in order to produce alloys of nominal compositions  $Mg_2Ni$  and  $Mg_2Ni_{0.95}Cu_{0.05}$ . Nanocrystalline phases based on the  $Mg_2Ni$  structure are produced after 21 hours of milling. As-milled powders were hydrided for 5 min at temperatures of 373, 423 and 473 K, under hydrogen pressures of between 0.69 and 2.07 MPa. The mass loss of the hydrided powders during thermogravimetric analysis was associated with hydrogen release. Maximum amounts of  $H_2$  release of 2.9 and 3.1 wt.% were obtained, respectively, for the  $Mg_2Ni$  and  $Mg_2Ni_{0.95}Cu_{0.05}$  samples hydrided at 473 K without prior activation. These are some of the most advantageous results ever reported concerning the behavior of the  $Mg_2Ni$  phase as a hydrogen storage material.

**Keywords:** Metal hydrides; hydrogen storage; nanocrystalline magnesium-base alloys; mechanical alloying.

Polvos elementales de Mg, Ni y Cu se sometieron a molienda de alta energía para producir aleaciones de composición nominal  $Mg_2Ni$  y  $Mg_2Ni_{0.95}Cu_{0.05}$ . Se obtuvieron fases nanocristalinas basadas en la estructura del  $Mg_2Ni$  después de 21 horas de molienda. Los polvos molidos se hidruraron durante 5 minutos a temperaturas de 373, 423 y 473 K y bajo presiones de hidrógeno en el intervalo de 0.69 a 2.07 MPa. La pérdida de masa durante el análisis termogravimétrico de los polvos hidrurados se asocia a la liberación de hidrógeno. Las cantidades máximas de hidrógeno liberado son 2.9 y 3.1% peso para muestras de  $Mg_2Ni$  y  $Mg_2Ni_{0.95}Cu_{0.05}$  hidruradas a 473 K, respectivamente. Estos resultados son de los más ventajosos que se han reportado sobre el desempeño de la fase  $Mg_2Ni$  como material para el almacenamiento de hidrógeno.

**Descriptores:** Hidruros metálicos; almacenamiento de hidrógeno; aleaciones nanocristalinas base Mg; aleado mecánico.

PACS: 81.07Bc; 82.33.Pt; 84.60.-h

## 1. Introduction

The use of hydrogen as a fuel and energy carrier depends to a large extent on the availability of adequate storage systems. Hydrogen storage compounds are one of several potentially useful materials for this purpose, and  $Mg_2Ni$  is one of the most promising candidates among them because of its relatively low density, low cost and high hydrogen storage capacity ( $\sim 3.6 \text{ wt.}\%$ ). Conventionally prepared polycrystalline  $Mg_2Ni$  absorbs hydrogen only at temperatures higher than about 520 K and under  $H_2$  pressures higher than about 1.5 MPa [1,2]. Moreover, polycrystalline  $Mg_2Ni$  must be activated by a series of heating-cooling cycles in a vacuum or in a hydrogen atmosphere before it can store significant quantities of hydrogen [1-6]. Several authors [e.g., 1,2,6-8] have pointed out that the hydriding properties of  $Mg_2Ni$  can be greatly enhanced by refining its microstructure (particle, grain or crystallite sizes). Also, the addition of many other substances, such as metal particles (e.g., Pd, Cu, V, Ni) [1,6,7,9-10], metal oxides [11-14], different forms of carbon [11,13,15,16], organic compounds [15,16] and even water [2], has been reported to improve the hydriding and dehydriding kinetics in Mg-based alloys. The present work is related to the production of  $Mg_2Ni-Ni$  and  $Mg_2(Ni,Cu)-Ni$  two-phase alloys by an optimized mechanical alloying (MA)

process and their enhanced hydrogen storage properties. Our work aimed at improving the reaction kinetics rather than modifying to any considerable extent their thermodynamic properties.

## 2. Experimental

Elemental Mg (99.9% nominal purity, particle size  $< 500 \mu\text{m}$ ), Ni (99.99%,  $< 100 \mu\text{m}$ ) and Cu (99.9%,  $< 75 \mu\text{m}$ ) were subjected to mechanical alloying (MA) in order to obtain alloys with nominal compositions (in atomic fractions)  $Mg_2Ni$  and  $Mg_2Ni_{0.95}Cu_{0.05}$ . Milling was performed in a high-energy SPEX vibratory mill, model 8000-D, using tool steel vials sealed under argon atmosphere. The products of MA were stored in argon-filled glass vials. Milling parameters such as total charge, ball-to-powder mass ratio (b/p), milling time and quantity of methanol (added as a process control agent) were varied in order to accelerate the formation of the desired  $Mg_2Ni$  phase and ensuring the existence of a nanocrystalline structure in the products. Optimized milling conditions are indicated in Table I.

Ball-milled powders, without prior activation treatment, were hydrided at temperatures of 373, 423 and 473 K under  $H_2$  pressures between 0.69 and 2.07 MPa. The hydriding process was carried out in a 50 ml – capacity stainless steel

TABLE I. Experimental milling conditions.

Sample	Nominal Composition	Milling	Methanol	Ball Mass	Number of	Ball to powder
	/ at. fraction	Time / hours	/ ml	/ g	balls	mass ratio
M1	Mg <sub>2</sub> Ni	5.5	0.5	8.3	6	5
M3	Mg <sub>2</sub> Ni	21	0.5	8.3	6	5
M15	Mg <sub>2</sub> Ni	21	0.25	8.3, 3.6, 1.0	4/3/5	10
M18	Mg <sub>2</sub> Ni <sub>0.95</sub> Cu <sub>0.05</sub>	21	0.25	8.3, 3.6, 1.0	4/3/5	10

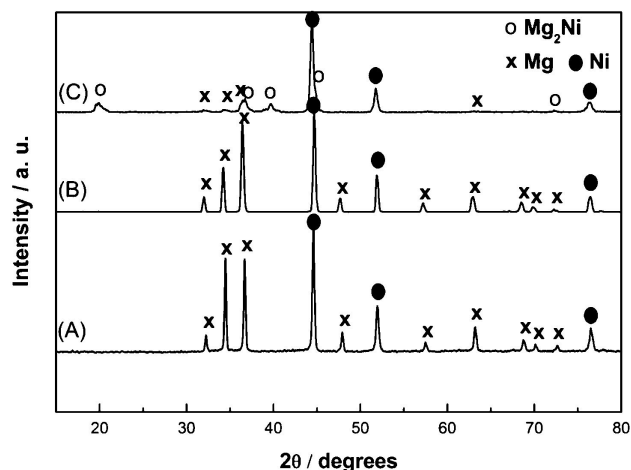


FIGURE 1. XRD patterns of Mg-Ni mixtures after different milling times (b/p = 5). (A) 0 hours, (B) 5.5 hours (sample M1) and (C) 21 hours (sample M3).

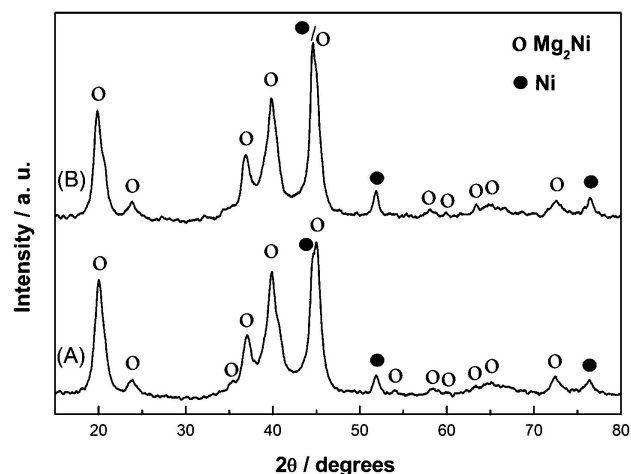


FIGURE 2. XRD patterns of Mg-Ni mixtures after a milling time of 21 hours (b/p = 10). (A) sample M15 and (B) sample M18 (with Cu addition).

reactor, by exposing the powder samples to gaseous H<sub>2</sub> (99.99% nominal purity) for only 5 minutes. Thermogravimetric analysis (TGA) was used to characterize the dehydrogenation process. Hydrided samples were heated from 293 to 673 K at 20 K min<sup>-1</sup> with N<sub>2</sub> as carrier gas. All powders were characterized by X-ray diffraction (XRD), scanning electron microscopy (SEM), energy-dispersive X-ray spectrometry (EDS), and transmission electron microscopy

(TEM). Quantitative phase analysis by the Rietveld method was performed on the XRD data from selected samples.

### 3. Results and discussion

#### 3.1. Mg<sub>2</sub>Ni/Ni alloys

Figure 1a shows the reference XRD pattern of the initial powder mixture before milling. In this pattern only Bragg reflections from elemental Mg and Ni are present. As shown by the corresponding XRD pattern in Fig. 1b, after 19.8 ks of MA (sample M1) there is still no evidence of formation of Mg<sub>2</sub>Ni; however, after 21 hours of MA (sample M3, Fig. 1c) the strongest reflection from Mg<sub>2</sub>Ni are clearly seen in addition to those from Ni and Mg. Also, sample M3 exhibits a marked broadening of all the diffraction peaks, suggesting the existence of microstrains and/or small crystallite sizes in the existing crystalline phases [17]. By doubling the b/p mass ratio and using balls of different sizes (see Table I) we were able to accelerate the formation of the Mg<sub>2</sub>Ni intermetallic compound, but leaving a small remanent quantity of Ni phase, which is beneficial in the decomposition reaction of the H<sub>2</sub> molecule. The two-phase, nanocrystalline nature of the final product is demonstrated by the XRD pattern obtained from sample M15, shown in Fig. 2a. The quantity of methanol added to sample M15 was reduced to 0.25 ml to avoid the production of a mixed carbide phase (MgNi<sub>3</sub>C<sub>x</sub>) [18].

#### 3.2. Mg<sub>2</sub>(Ni,Cu)/Ni alloys

The alloys with nominal composition Mg<sub>2</sub>Ni<sub>0.95</sub>Cu<sub>0.05</sub> were prepared under the optimized milling conditions described above. The corresponding XRD pattern shown in Fig. 2b exhibits Bragg reflection from Mg<sub>2</sub>Ni and Ni only. Considerable broadening of the diffraction peaks is also observed in this XRD pattern, suggesting the existence of microstrains and/or nanometric-scale crystallite size in the as-milled material. The nanocrystalline structure of the as-milled samples was indeed verified by TEM observations. Figure 3a shows a dark-field TEM image from a powder particle from sample M18 in which crystallites of sizes smaller than about 25 nm are clearly displayed in the dark-field imaging mode. The corresponding selected-area electron diffraction pattern given in Fig. 3b shows the indexed Ni and Mg<sub>2</sub>Ni rings, thus confirming the phase identification done by XRD.

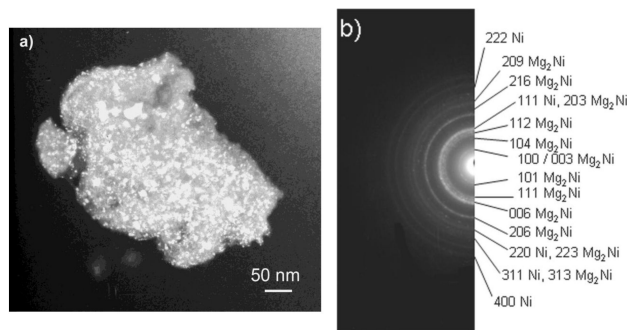


FIGURE 3. (a) Dark-field TEM image of a particle from sample M18 and (b) corresponding selected-area electron diffraction pattern.

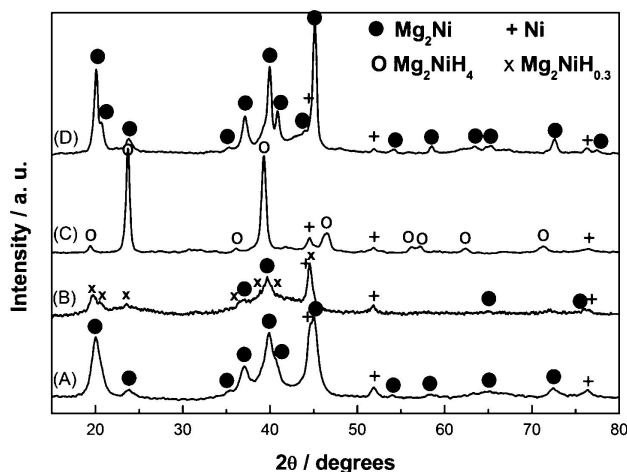


FIGURE 4. XRD patterns of sample M15: (A) as-milled, (B) hydrided at 423 K and  $p_{H_2} = 0.97 \text{ MPa}$ , (C) hydrided at 473 K and  $P = 1.24 \text{ MPa}$  and (D) dehydrided by TGA.

The milling parameters applied to samples M15 and M18 assured the production of only  $Mg_2Ni$  and residual Ni, so that no further milling was deemed necessary to attain our goals. The Rietveld analysis of the XRD data resulted in practically identical results of phase quantification for both samples: 93 wt.%  $Mg_2Ni$  and 7 wt.% Ni. It is worth noting that the formation of  $Mg_2Ni$  by MA was accomplished in only 21 hours, in contrast to previous works [1,6,11,19] in which milling times as long as 66-100 hours are reported in order to produce this intermetallic compound. This is the result of an adequate design of the milling operation in the present work.

### 3.3. Hydriding and dehydriding characteristics

Hydrided and subsequently dehydrided powders from samples M15 and M18 were also analyzed by XRD. Figure 4a shows again, as a reference, the XRD pattern of as-milled sample M15 in which only  $Mg_2Ni$  and Ni phases are present. After hydriding under the conditions  $P = 0.97 \text{ MPa}$  and  $T = 423 \text{ K}$ , the corresponding diffraction pattern (Fig. 4b) shows diffraction peaks belonging to  $Mg_2NiH_{0.3}$ ,  $Mg_2Ni$  and

Ni, in the amounts of 53 wt.%, 40 wt.% and 7 wt.%, respectively. From these results it can be inferred that the hydriding reaction was not complete, with approximately 40 wt.% of  $Mg_2Ni$  still remaining. On subsequent dehydridation in the TGA apparatus, this sample released 1.9 wt.% of hydrogen. Hydriding of sample M15 at a higher temperature and pressure ( $P = 1.24 \text{ MPa}$ ,  $T = 473 \text{ K}$ ) produced a larger proportion of the intermetallic hydrides, judging by the relative intensities of their peaks in the corresponding XRD pattern, Fig. 4c. In this figure only Bragg reflection from  $Mg_2NiH_{4-LT}$  (low temperature phase) and residual Ni are identified. Phase quantification in this sample by the Rietveld method reported 78 wt.%  $Mg_2NiH_{4-LT}$ , 15 wt.%  $Mg_2NiH_{0.3}$ , the balance being Ni. During TGA this sample released 2.7 wt.% of hydrogen.

Figure 4d shows the corresponding XRD pattern of the dehydrided powders from sample M15, in which diffraction peaks from  $Mg_2Ni$  and Ni have reappeared, thus confirming the reversible nature of the hydriding/dehydriding process. Phase quantification of these dehydrided powders reported 4 wt.% Ni, 81 wt.%  $Mg_2Ni$  and 15 wt.%  $Mg_2NiH_{0.3}$  (Bragg reflection from  $Mg_2NiH_{0.3}$  are not evident in Fig. 4d); obviously, in this case the dehydriding reaction was not completed. Figure 4b still shows considerable broadening of the diffraction peaks, even though the samples were heated to 423 K during hydriding. In comparison, the diffraction peaks in Figs. 4b-c are slightly narrower than those in the as-milled sample (Fig. 4a), probably because crystallite growth and/or microstrain release occurred after heating the samples to temperatures of up to 673 K (Fig. 4d). Nevertheless, the nanocrystalline structure of the as-milled samples remains at least to some extent in the hydrided/dehydrided specimens, which is an important issue for ensuring reproducibility of hydriding characteristics under cycling conditions.

Analogous XRD results were obtained for sample M18, as seen in Fig. 5. A specimen hydrided at 373 K and  $P = 1.72 \text{ MPa}$  (Fig. 5b) shows Bragg reflection associated with  $Mg_2NiH_{0.3}$ ,  $Mg_2Ni$  and Ni. These phases were quantified as 38 wt.%, 54 wt.% and 8 wt.%, respectively. As in the previous case, only reflection from  $Mg_2NiH_{0.3}$  are present after hydriding at a relatively low temperature and pressure. If the hydriding reaction takes place at a higher temperature (473 K and  $P = 1.66 \text{ MPa}$ ) diffraction peaks of  $Mg_2NiH_{4-LT}$  (72 wt.%) are also present, along with those of  $Mg_2NiH_{0.3}$  (19 wt.%), and Ni (9 wt.%), as shown in Fig. 5c. The quantitative analysis results of the hydrided and dehydrided powder obtained by the Rietveld method are summarized in Table II. The figure of merit ( $R_{wp}$ ) of the Rietveld refinement are also given in this Table. Large values of  $R_{wp}$  were obtained ( $4 < R_{wp} < 15$ ), due to the intrinsic difficulty of refining broad and not completely well-defined diffraction peaks. Nevertheless, for the quantitative estimation of phase content, the  $R_{wp}$  values shown in Table II are considered suitable.

TABLE II. Phase quantification of selected hydrided and dehydrided samples (Rietveld Method) in wt. %.

Sample	(Numbers in parenthesis are figure of merit, $R_{wp}$ , of the Rietveld refinement)				Comments
	Ni	Mg <sub>2</sub> Ni	Mg <sub>2</sub> NiH <sub>4</sub> -LT	Mg <sub>2</sub> NiH <sub>0.3</sub>	
M15	7(4)	93(5)	—	—	As-milled
M15 (hydrided)	7(10)	40(13)	—	53(15)	Hydrided at 0.97 MPa and 423 K, 1.9 wt.% H <sub>2</sub> (released)
M15 (hydrided)	7(5)	—	78(10)	15(12)	Hydrided at 1.24 MPa and 423 K, 2.7 wt.% H <sub>2</sub> (released)
M15 (dehydrided)	4(7)	81(9)	—	15(13)	Dehydrided by TGA heating from 273 to 673 K
M18	7(4)	93(6)	—	—	As-milled
M18 (hydrided)	8(9)	54(10)	—	38(6)	Hydrided at 1.79 MPa and 373 K, 1.7 wt.% H <sub>2</sub> (released)
M18 (hydrided)	9(7)	—	72(12)	19(15)	Hydrided at 1.66 MPa and 473 K, 3.0 wt.% H <sub>2</sub> (released)

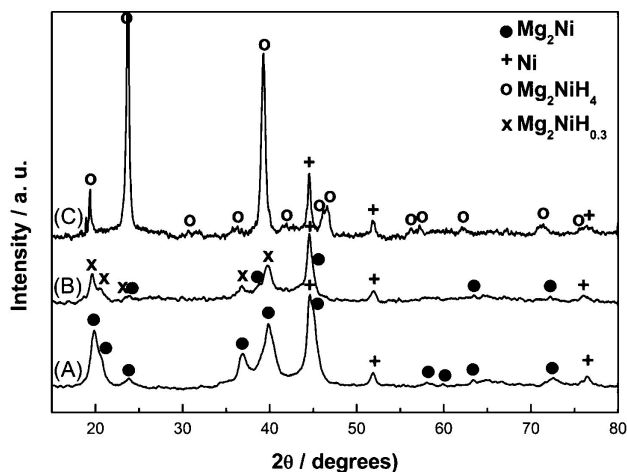
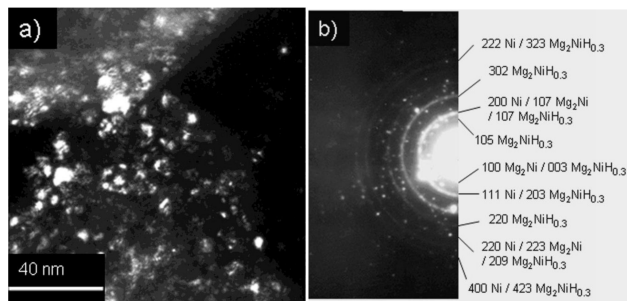
FIGURE 5. XRD patterns of sample M18: (A) as-milled, (B) hydrided at 373 K and  $p_{H_2} = 1.72$  MPa and (C) hydrided at 473 K and  $p_{H_2} = 1.66$  MPa.

FIGURE 6. (a) Dark-field TEM image of a particle from hydrided sample M15 and (b) corresponding selected-area electron diffraction pattern.

From the considerable broadening of the diffraction peaks shown in Figs. 5b and 5c, nanometric-scale crystallites in the hydrided products can be inferred (remaining microstrains are unlikely because of the exposure to high temperatures).

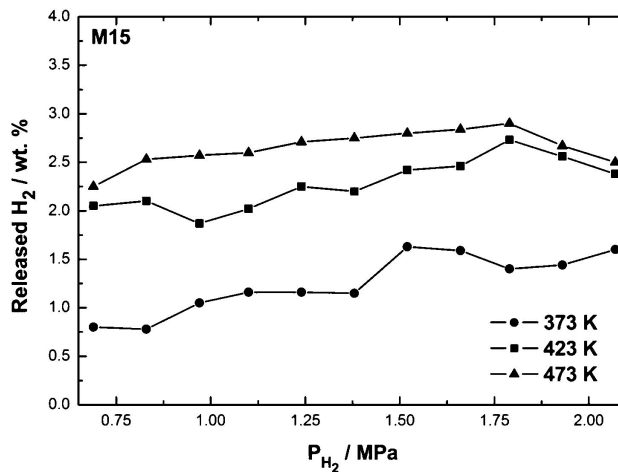
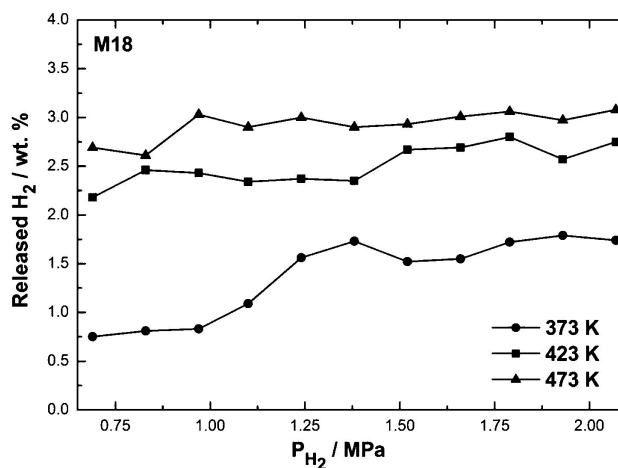
FIGURE 7. Weight percentage of H<sub>2</sub> released by heating during TGA of hydrided powders from sample M15.FIGURE 8. Weight percentage of H<sub>2</sub> released by heating during TGA of hydrided powders from sample M18.

TABLE III. Maximum weight percentages of H<sub>2</sub> estimated from TGA.

(Numbers in parenthesis are the corresponding hydriding pressures)		
Temperature / K	Sample M15	Sample M18
373	1.6(2.1 MPa)	1.8 (1.9 MPa)
423	2.7(1.8 MPa)	2.8 (1.8 MPa)
473	2.9(1.8 MPa)	3.1 (2.1 MPa)

Evidence of the nanocrystalline structure in the hydrided powders is given in Fig. 6a, in which a dark-field TEM image from a powder particle of a hydrided sample of alloy M15 is shown. Crystallites of less than 15 nm in size can be observed in this image, even after the sample was heated up to 423 K. The corresponding selected-area electron diffraction pattern is shown in Fig. 6b. Diffraction rings belonging to Mg<sub>2</sub>NiH<sub>0.3</sub>, Mg<sub>2</sub>Ni and Ni have been indexed in this pattern, confirming the phase analysis deduced from the XRD data.

The weight percentages of H<sub>2</sub> released during TGA from hydrided samples of alloy M15 and alloy M18 (Mg<sub>2</sub>Ni and Ni were the existing phases in both as-milled samples) are shown in Figs. 7 and 8, respectively, for reaction temperatures of 373, 423 and 473 K. From these plots it can be deduced that the higher the hydriding temperature, the higher the H<sub>2</sub> content in the sample and the quantity of gaseous H<sub>2</sub> released during TGA. However, the relative increase in hydrogen release (and, assumedly, in H<sub>2</sub> uptake) when the hydriding temperature goes from 373 to 423 K is more evident than the increase from 423 to 473 K. On the other hand, regarding the hydriding pressure, in all cases the general tendency is towards higher hydrogen uptake with increasing pressure, but the effect is more noticeable at 373 K than at 423 and 473 K. From Figs. 7 and 8, it is also observed that the dehydriding characteristics of the Cu-containing Mg<sub>2</sub>Ni/Ni alloy are somewhat better than those found in the samples without Cu addition. For example, for a hydriding temperature of 373 K, 1.5 wt.% of H<sub>2</sub> is released by using P > 1.5 MPa in the hydriding operation of the Mg<sub>2</sub>Ni/Ni alloy, while the same amount of H<sub>2</sub> is released by hydriding the Cu-containing alloy under P ~ 1.25 MPa. Similarly, 2.5 wt.% of

H<sub>2</sub> is released from sample M18 by hydriding at P ~ 0.8 MPa and 423 K, while for sample M15 the same amount of H<sub>2</sub> release required a hydriding pressure of P > 1.75 MPa. These pressures may indicate a change in the thermodynamics of hydride formation in the Cu-containing alloy, meaning that a mixed (Mg-Cu) hydride could be more stable than MgH<sub>2</sub> at the temperatures used in our experiments.

Finally, under optimum conditions in our experiments, the maximum amount of H<sub>2</sub> release was about 3.1 wt.% in the Cu-containing alloy, while the Mg<sub>2</sub>Ni/Ni alloy released a maximum amount of about 2.9 wt.%.

Maximum weight percentages of H<sub>2</sub> released during TGA are summarized in Table III. It is worth comparing these data to the results reported by other authors. For example, using a hydriding temperature of 423 K, sample M15 released a maximum of 2.7 wt.% of hydrogen and the corresponding value for sample M18 was 2.8 wt.%; in contrast, at the same temperature Janot *et al.* [11] reported a hydrogen release of 1.6 wt.% from hydrided Mg<sub>2</sub>Ni (also produced by milling). Furthermore, under the same conditions these authors reported hydrogen releases from Mg<sub>2</sub>Ni-graphite and Pd-coated Mg<sub>2</sub>Ni-graphite composites of 2.6 and 2.8 wt.%, respectively, that is, about the same amount as the simpler materials produced in our experiments.

#### 4. Conclusions

By a suitable choice of milling parameters, two-phase nanocrystalline Mg<sub>2</sub>Ni/Ni alloys were produced by mechanical alloying in 21 hours, a much shorter processing time than previously reported. Powders hydrided for only 5 min at 473 K and 2.07 MPa of H<sub>2</sub> pressure showed a maximum amount of released H<sub>2</sub> of 2.9 and 3.1 wt.% for Mg<sub>2</sub>Ni/Ni and Mg<sub>2</sub>(Ni,Cu)/Ni alloys, respectively. The addition of Cu considerably reduced the pressure needed to store a given quantity of H<sub>2</sub>, an observation that is taken to indicate the formation of a mixed (Mg-Cu) hydride, thermodynamically more stable than MgH<sub>2</sub>. Considering the short hydriding time (5 min) used, these results indicate a clear improvement in the hydriding characteristics for Mg<sub>2</sub>Ni-type materials.

\* Corresponding author: e-mail: palacios.af@gmail.com

- L. Zaluski, A. Zaluska, and J.O. Ström-Olsen, *J. Alloy. Compd.* (1995) 245.
- J.K. Lomness, M.D. Hampton, and L.A. Giannuzzi, *Int. J. Hydrogen Energy* **27** (2002) 915.
- P. Zolliker and K. Yvon, *J. Less-Common Met.* **115** (1986) 65.
- D. Noreus and P.E. Werner, *J. Less-Common Met.* **97** (1984) 215.
- M.Y. Song, E.I. Ivanov, B. Darriet, M. Pezat, and P. Hagemuler, *Int. J. Hydrogen Energy* **10** (1985) 169.
- A.K. Singh and O.N. Srivastava, *J. Alloy. Compd.* **1995** 227 63.
- T. Spassov, P. Solsona, S. Bliznakov, S. Suriñach, and M.D. Baró, *J. Alloy. Compd.* **356-357** (2003) 639.
- H. Niu and D.O. Northwood, *Int. J. Hydrogen Energy* **27** (2002) 69.
- H. Yukawa, T. Matsumura, and M. Morinaga, *J. Alloy. Compd.* (1999) 227.
- R. Yang *et al.*, *Acta Mater.* **50** (2002) 109.
- R. Janot, L. Aymard, A. Rougier, G.A. Nazri, and J.M. Tarascon, *J. Mater. Res.* **18** (2003) 1749.

12. S. Hwang, C. Nishimura and P.G. McCormick, *Mat. Sci. and Eng. A* **318** (2001) 22.
13. S. Nohara, H. Inoue, Y. Fukumoto, and C. Iwakura, *J. Alloy. Compd.* **252** (1997) L16.
14. J.L. Bobet and B. Chevalier, *J. Mat. Sci.* **39** (2004) 5243.
15. H. Imamura *et al.*, *Acta Mater.* **51** (2003) 6407.
16. H. Imamura *et al.*, *J. Alloy. Compd.* **386** (2005) 211.
17. G.K. Williamson and H. Hall, *Acta Metall.* **1** (1953) 22.
18. A. Palacios-Lazcano, J.G. Cabañas-Moreno, and F. Cruz-Gandarilla, *Scripta Mater* **52** (2005) 571.
19. T. Aizawa, T. Kuji, and H. Nakano, *J. Alloy. Compd.* **291** (1999) 248.